The Astrophysical Journal Letters, 850:L24 (5pp), 2017 December 1 https://doi.org/10.3847/2041-8213/aa991d


# Lessons from the Short GRB 170817A: The First Gravitational-wave Detection of a Binary Neutron Star Merger

Jonathan Granot[1], Dafne Guetta[2], and Ramandeep Gill[1,3]
[1] Department of Natural Sciences, The Open University of Israel, 1 University Road, POB 808, Raanana 4353701, Israel
[2] Department of Physics and Optical Engineering, ORT Braude College, Karmiel 21982, Israel
[3] Physics Department, Ben-Gurion University, P.O.B. 653, Beer-Sheva 84105, Israel
*Received 2017 October 18; revised 2017 November 5; accepted 2017 November 6; published 2017 November 22*

## Abstract

The first, long-awaited, detection of a gravitational-wave (GW) signal from the merger of a binary neutron star (NS–NS) system was finally achieved (GW170817) and was also accompanied by an electromagnetic counterpart —the short-duration gamma-ray burst (GRB) 170817A. It occurred in the nearby ($D \approx 40$ Mpc) elliptical galaxy NGC 4993 and showed optical, IR, and UV emission from half a day up to weeks after the event, as well as late-time X-ray (at $\geqslant$8.9 days) and radio (at $\geqslant$16.4 days) emission. There was a delay of $\Delta t \approx 1.74$ s between the GW merger chirp signal and the prompt GRB emission onset, and an upper limit of $\theta_{\rm obs} < 28^\circ$ was set on the viewing angle w.r.t the jet's symmetry axis from the GW signal. In this letter we examine some of the implications of these groundbreaking observations. The delay $\Delta t$ sets an upper limit on the prompt GRB emission radius, $R_\gamma \lesssim 2c\Delta t/(\theta_{\rm obs} - \theta_0)^2$, for a jet with sharp edges at an angle $\theta_0 < \theta_{\rm obs}$. GRB 170817A's relatively low isotropic equivalent $\gamma$-ray energy output may suggest a viewing angle slightly outside the jet's sharp edge, $\theta_{\rm obs} - \theta_0 \sim (0.05 - 0.1)(\Gamma/100)^{-1}$, but its peak $\nu F_\nu$ photon energy and afterglow emission suggest instead that the jet does not have sharp edges and the prompt emission was dominated by less energetic material along our line of sight, at $\theta_{\rm obs} \gtrsim 2\theta_0$. Finally, we consider the type of remnant that is produced by the NS–NS merger and find that a relatively long-lived (>2 s) massive NS is strongly disfavored, while a hyper-massive NS of lifetime $\sim$1 s appears to be somewhat favored over the direct formation of a black hole.

*Key words:* gamma-ray burst: general – gravitational waves – stars: neutron

## 1. Introduction

The first discovery of gravitational waves (GWs) from two coalescing black holes (BHs) by the Advanced Laser Interferometer Gravitational-wave Observatory (LIGO) ushered in a new era of GW astronomy (Abbott et al. 2016a). It was soon followed by three other BH–BH mergers that firmly established LIGO's sensitivity to robustly detect such sources out to $\sim$Gpc distances. LIGO can also detect GWs from compact binary mergers involving neutron stars (NSs), NS–NS and NS–BH, at a volume-weighted mean distance of $\sim$70 Mpc and $\sim$110 Mpc, respectively, and set an upper limit of $12,600\ {\rm Gpc^{-3}\ yr^{-1}}$ on the NS–NS merger rate (90% CL; Abbott et al. 2016b).

An electromagnetic (EM) counterpart to the GW signal from a BH–BH merger is not expected (in most scenarios). However, its detection is of great importance in NS–NS or NS–BH mergers, which have been posited to be the progenitors of short-hard gamma-ray bursts (SGRBs; e.g., Eichler et al. 1989; Narayan et al. 1992). An NS–NS merger likely leads to the formation of a BH, possibly preceded by a short-lived hyper-massive NS (e.g., Baumgarte et al. 2000). Accretion onto the BH launches a relativistic jet reaching bulk Lorentz factors $\Gamma \gtrsim 100$ and powering an SGRB—a short ($\lesssim$2 s) intense flash of $\gamma$-rays with a typical ($\nu F_\nu$-peak) photon energy $E_{\rm pk} \sim 400$ keV and total isotropic equivalent energy release $E_{\gamma,{\rm iso}} \simeq 10^{49}$–$10^{51}$ erg (Nakar 2007; Berger 2014). On the other hand, long-soft GRBs are known to originate from the death of massive stars, via their association with star-forming regions and type Ic core-collapse supernovae (e.g., Woosley & Bloom 2006).

The unprecedented observation of an SGRB (Abbott et al. 2017a; von Kienlin et al. 2017) coincident with the detection of GWs from coalescing binary NSs (Abbott et al. 2017b) in an elliptical galaxy presents the long-awaited "smoking gun" that binary NS mergers give rise to SGRBs. Rapid follow-up observations by detectors across the EM spectrum (Abbott et al. 2017c) both increase the positional accuracy of the source in the host galaxy and yield critical information regarding jet geometry, merger ejecta, and *r*-process elements (e.g., Rosswog et al. 2013).

In Section 2, the delay between the GW and SGRB signals is used to constrain the location of the $\gamma$-ray emission region. In Section 3, the prompt $\gamma$-ray emission properties are used to constrain the GRB jet's angular structure and our viewing angle $\theta_{\rm obs}$ from the jet's symmetry axis. The constraints on the type of remnant produced by the NS–NS merger are discussed in Section 4. Finally, the implications of this work are discussed in Section 5.

## 2. The Time Delay between the GW Signal and SGRB: An Upper Limit on the Emission Radius

A delay of $\Delta t = 1.74 \pm 0.05$ s was found between the binary merger GW chirp signal and GRB 170817A's $\gamma$-ray emission onset (Abbott et al. 2017a). Such a delay can arise from one or more causes and may provide important information on the merging system and the merger process (e.g., Abbott et al. 2017a; Ioka & Nakamura 2017; Murguia-Berthier et al. 2017). Moreover, the GW signal and known distance to the host galaxy set an upper limit on the viewing angle of $\theta_{\rm obs} < 28^\circ \approx 0.49$ rad (Abbott et al. 2017b).

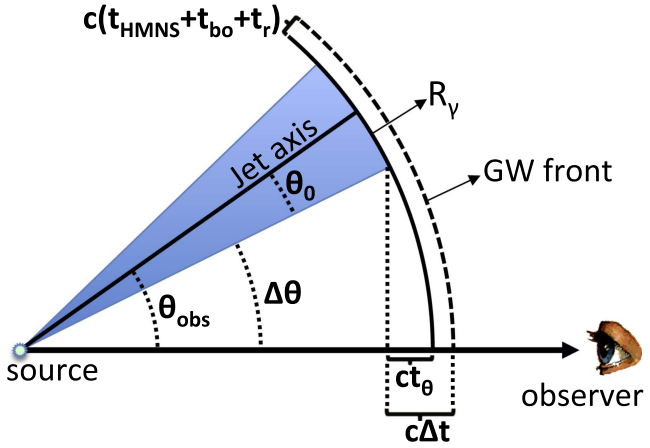


**Figure 1.** Illustration of the $\gamma$-ray to GW geometrical time delay $t_\theta$ for a jet viewed from outside of its aperture.

One possible cause for such a delay is the formation of a short-lived, $t_{\rm HMNS} \lesssim 1$ s, hyper-massive NS, whose collapse forms a BH surrounded by an accretion disk that launches a relativistic jet. In order to produce a GRB, the jet must first bore its way through the dynamical ejecta and/or neutrino-driven wind that was launched during $t_{\rm HMNS}$, causing a time delay of $t_{\rm bo}$, which may typically be a good fraction of a second (e.g., Moharana & Piran 2017; Nakar & Piran 2017). Once the jet breaks out of this wind or outflow, it quickly accelerates to ultra-relativistic speeds, where compactness arguments suggest that its Lorentz factor during the prompt $\gamma$-ray emission, at a distance of $R_\gamma$ from the central source, is $\Gamma \gtrsim 100$. The delay $t_r$ in the $\gamma$-ray emission onset for an on-axis observer that is caused by this acceleration phase and a possible coasting phase until the jet reaches $R_\gamma$, due to the jet's motion along the radial direction at speeds slightly less than $c$, is typically negligible (usually $t_r \lesssim R_\gamma/2c\Gamma^2 = 1.7 R_{\gamma,13}/\Gamma_{2.5}^2$ ms[4]).

When the outflow in the jet reaches the $\gamma$-ray emission radius, $R_\gamma$, it radiates the prompt GRB. For a jet viewed off-axis from $\theta_{\rm obs} > \theta_0$ this angular offset causes a geometrical delay because of the the additional path length of the radiation from the edge of the jet closest to the observer compared to an on-axis observer (see Figure 1),

$$t_\theta = \frac{R_\gamma}{c}[1 - \cos(\Delta\theta)] \approx \frac{R_\gamma}{2c}\Delta\theta^2 = 1.67 R_{\gamma,13}\Delta\theta_{-1}^2 \,{\rm s}, \quad (1)$$

where $\Delta\theta \equiv \theta_{\rm obs} - \theta_0 = 0.1\Delta\theta_{-1}$. Altogether, the total delay is the sum of all the different causes, $\Delta t \geqslant t_{\rm HMNS} + t_{\rm bo} + t_r + t_\theta > t_\theta$. Therefore, one can use the fact that $\Delta t > t_\theta \approx R_\gamma \Delta\theta^2/2c$ to set an upper limit on $R_\gamma$,

$$R_\gamma < \frac{c\Delta t}{1 - \cos(\Delta\theta)} \approx \frac{2c\Delta t}{\Delta\theta^2} = 6 \times 10^{12}\left(\frac{\Delta t}{1\ {\rm s}}\right)\Delta\theta_{-1}^{-2}\ {\rm cm}. \quad (2)$$

This upper limit $R_{\gamma,\rm max}$ on $R_\gamma$ is plotted in Figure 2 for $(\Delta t, \theta_0) = (0.5\ {\rm s}, 0)$, $(1.74\ {\rm s}, 0)$, $(1.74\ {\rm s}, 0.1)$, and $(1.74\ {\rm s}, 0.2)$. The afterglow lightcurve fits suggest $\Delta\theta \gtrsim 0.2$ (Granot et al. 2017), as illustrated by the vertical lines in Figure 2. Together with the measured $\Delta t$ this implies $R_\gamma \lesssim 1.7 \times 10^{12}(\Delta\theta/0.25)^{-2}$ cm. Such a limit is very restrictive for models

[4] We adopt the convention $Q_x = Q/10^x$ (cgs units).

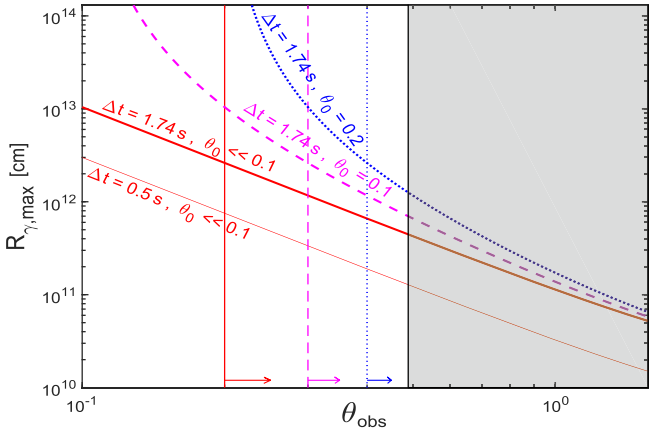


**Figure 2.** Upper limit $R_{\gamma,\rm max}$ on the $\gamma$-ray emission radius from the geometrical time delay, $t_\theta$, as a function of the viewing angle, $\theta_{\rm obs}$, for four sets of $(\Delta t, \theta_0)$ values. The corresponding vertical lines are tentative lower limits on $\theta_{\rm obs}$ from the fact that afterglow fits suggest $\Delta\theta \gtrsim 0.2$. The gray region is excluded by the GW signal.

of the GRB prompt emission and outflow acceleration. Note that any estimate or lower limit on the other time delays besides $t_\theta$ that contribute to $\Delta t$ could make this upper limit on $R_\gamma$ even stricter. A long-lived HMNS, $t_{\rm HMNS} \gtrsim 0.3$–1 s, for which one might expect $t_{\rm bo} \gtrsim 0.5$ s would imply a lower $t_\theta \lesssim 0.5$–1 s (see the thin red line in Figure 2 for $t_\theta = 0.5$ s as an illustration of such a case).

## 3. Constraining the Viewing Angle from the Prompt GRB Emission

Since the prompt GRB emission was observed, we are either (i) within the jet's initial aperture ($\theta_{\rm obs} < \theta_0$) or beaming cone ($\theta_{\rm obs} < \theta_0 + 1/\Gamma$); (ii) slightly outside of a sharp-edged jet, $\theta_{\rm obs} > \theta_0$, but $\Gamma\Delta\theta$ is not loo large for the prompt emission to be detectable; or (iii) well outside the core of a jet ($\theta_{\rm obs} \gtrsim 2\theta_0$) that (more realistically) does not have very sharp edges and the prompt GRB is produced by relativistic outflow along our line of sight (for further discussion of structured jets and off-axis emission see, e.g., Salafia et al. 2015; Alexander et al. 2017; Haggard et al. 2017; Ioka & Nakamura 2017; Jin et al. 2017; Kathirgamaraju et al. 2017; Lazzati et al. 2017a, 2017b; Murguia-Berthier et al. 2017). An alternative that is not discussed here in detail is that the prompt GRB and possibly the afterglow arise from the breakout of a mildly relativistic cocoon (Abbott et al. 2017a; Bromberg et al. 2017; Evans et al. 2017; Gottlieb et al. 2017; Kasliwal et al. 2017; Troja et al. 2017).

In case (i) a bright and usually highly variable prompt $\gamma$-ray emission is expected, with relatively high values of the isotropic equivalent $\gamma$-ray energy output, $E_{\gamma,\rm iso}$, and peak photon energy, $E_{\rm p}$. GRB 170817A had a fluence of $f = (2.8 \pm 0.2) \times 10^{-7}$ erg cm$^{-2}$ (10–1000 keV) corresponding to $E_{\gamma,\rm iso} = (5.36 \pm 0.38) \times 10^{46} D_{40\,\rm Mpc}^2$ erg and $E_{\rm p} = 82 \pm 21$ keV (von Kienlin et al. 2017). The initial half-second spike had $E_{\rm p} = 185 \pm 62$ keV, while the softer tail had $E_{\rm p} = 40 \pm 6$ keV and a blackbody spectrum (Abbott et al. 2017c). For SGRBs with known redshifts, typically, $E_{\gamma,\rm iso} \sim 10^{49}$–$10^{51}$ erg, i.e., ~3–4 decades above GRB 170817A, and an intrinsic $\langle(1+z)E_p\rangle \sim 500$–600 keV, several times larger than in GRB 170817A. The low $E_{\gamma,\rm iso}$ and $E_{\rm p}$ in GRB 170817A suggest a line of sight is outside of the jet, $\theta_{\rm obs} > \theta_0$, arguing

against case (i) above ($\theta_{\rm obs} > \theta_0$ also corresponds to most of the total solid angle for narrow jets and is thus more likely for events associated with a binary merger GW signal), as do the afterglow observations.

In case (ii), the observed low $E_{\gamma,\rm iso}$ and $E_{\rm p}$ values are caused by a viewing angle outside of the jet's initial aperture, $\theta_{\rm obs} > \theta_0$. For a uniform jet with sharp edges the ratio of off-axis to on-axis $E_{\rm p}$ and $E_{\gamma,\rm iso}$ are (Granot et al. 2002, 2005; Granot & Ramirez-Ruiz 2012)

$$\frac{E_{\rm p}(\theta_{\rm obs})}{E_{\rm p}(0)} \equiv a \approx \begin{cases} 1 & \theta_{\rm obs} < \theta_0, \\ \frac{1}{1+(\Gamma\Delta\theta)^2} \sim (\Gamma\Delta\theta)^{-2} & \theta_{\rm obs} > \theta_0, \end{cases} \quad (3)$$

$$\frac{E_{\gamma,\rm iso}(\theta_{\rm obs})}{E_{\gamma,\rm iso}(0)} \approx \begin{cases} 1 & \theta_{\rm obs} < \theta_0, \\ a^2 \sim (\Gamma\Delta\theta)^{-4} & 1 < \frac{\theta_{\rm obs}}{\theta_0} < 2, \\ \frac{(\Gamma\theta_0)^2}{(\Gamma\Delta\theta)^6} \sim \frac{(\Gamma\theta_0)^2}{(\Gamma\theta_{\rm obs})^6} & \theta_{\rm obs} > 2\theta_0, \end{cases} \quad (4)$$

where we assume that $\Gamma\theta_0 \gg 1$, as is inferred for GRBs. For $1 < \theta_{\rm obs}/\theta_0 < 2$, $E_{\gamma,\rm iso}(\theta_{\rm obs})/E_{\gamma,\rm iso}(0) \sim (\Gamma\Delta\theta)^{-4}$ already reaches its inferred value of $\sim 10^{-4}$–$10^{-3}$ for $\Delta\theta \sim (0.05\text{–}0.1)\,(100/\Gamma) \lesssim 0.05$–$0.1$, where $\Gamma \gtrsim 100$ for GRBs, i.e., in case (ii), we are observing only slightly outside the jet's outer edge. For GRB 170817A this implies $E_{\rm p}(\theta_{\rm obs})/E_{\rm p}(0) = a = [E_{\gamma,\rm iso}(\theta_{\rm obs})/E_{\gamma,\rm iso}(0)]^{1/2} \sim 0.01$–$0.03$ and hence $E_{\rm p}(0) \sim$ 3–8 MeV (or ∼5–20 MeV for the main half-second initial spike), which is unusually high for an SGRB of typical $E_{\gamma,\rm iso}$.

Case (iii) allows large off-axis viewing angles $\theta_{\rm obs} \gtrsim 2\theta_0$ for which the afterglow emission from the jet's core peaks and joins the post jet-break on-axis lightcurve at $t_{\rm peak} \propto \theta_{\rm obs}^2$ (e.g., Granot et al. 2002; Nakar et al. 2002). Moreover, in this case we also expect in addition to this off-axis emission from the jet's core a contribution to the afterglow lightcurve from the material along the line of sight after it produces the prompt GRB. The latter may dominate at early times before $t_{\rm peak}(\theta_{\rm obs})$, while the emission from the jet's energetic core ($\theta < \theta_0$) is still strongly beamed away from the observer. At $t \gtrsim t_{\rm peak}$ the line of sight enters the beaming cone of the jet's core so that its larger energy causes its emission to dominate over that from the less energetic material along the line of sight at $t \gtrsim t_{\rm peak}$. Therefore, in case (iii) a shallower rise to the peak flux at $t_{\rm peak}$ may be expected (e.g., Granot et al. 2002; Granot & Kumar 2003; Eichler & Granot 2006).

The early afterglow emission from material along our line of sight in case (iii) may be estimated by assuming spherical emission with the local isotropic equivalent kinetic energy $E_{\rm k,iso} \sim E_{\gamma,\rm iso} \approx 5.4 \times 10^{46} D_{40\,\rm MPc}^2$ erg. The latter assumption is reasonable at sufficiently early times when one expects that $E_{\rm k,iso}$ has not greatly changed from its initial value. The flux densities in the relevant power-law segments of the spectrum are (Granot & Sari 2002; after the local deceleration time)

$$F_{\nu>\nu_c,\nu_m} = 0.60\epsilon_{e,-1}^{p-1}\epsilon_{B,-2}^{\frac{p-2}{4}} t_{\rm days}^{(2-3p)/4} \nu_{14.7}^{-p/2}\ \mu{\rm Jy}, \quad (5)$$

$$F_{\nu_m<\nu<\nu_c} = 7.6\epsilon_{e,-1}^{p-1}\epsilon_{B,-2}^{\frac{p+1}{4}} n_0^{1/2} t_{\rm days}^{\frac{3-3p}{4}} \nu_{14.7}^{\frac{1-p}{2}}\ {\rm nJy}, \quad (6)$$

$$F_{\nu_a<\nu<\nu_m<\nu_c} = 156\epsilon_{e,-1}^{-\frac{2}{3}}\epsilon_{B,-2}^{1/3} n_0^{\frac{1}{2}} t_{\rm days}^{1/2} \nu_{9.93}^{1/3}\ \mu{\rm Jy}, \quad (7)$$

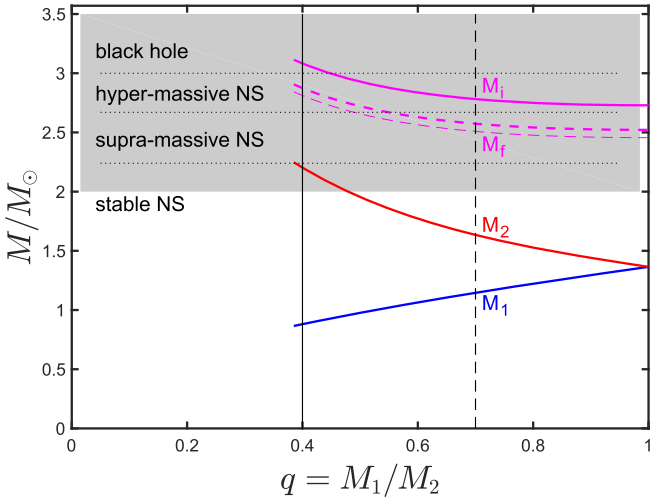


**Figure 3.** Possible pre-merger masses of the two NSs, $M_1$ (in blue) and $M_2$ (in red), as a function of their mass ratio $q \equiv M_1/M_2 \leqslant 1$, given the measured chirp mass, $\mathcal{M} \equiv (M_1M_2)^{3/5}(M_1+M_2)^{-1/5} = 1.188^{+0.004}_{-0.002}\,M_\odot$. Also shown are the system's pre-merger total (gravitational) mass, $M_i$, before (solid magenta line) and after (dashed magenta lines) accounting for losses due to mass ejection (of 0.01 $M_\odot$—thick line, or 0.1 $M_\odot$—thin line), gravity waves, and neutrinos during the merger (as described in the text). The vertical thin lines indicate the lower limit on $q$ from the GW signal, for two different priors on the NSs' aligned spin components ($|\chi| \leqslant 0.89$ and $|\chi| \leqslant 0.05$ for the solid and dashed lines, respectively; see Abbott et al. 2017b). Also shown schematically are the possible outcomes, in order of increasing final mass range: a stable NS, an SMNS, an HMNS, and a BH. The shaded region above 2 $M_\odot$ indicates the uncertainty in the mass limits dividing the different types of remnants.

with the numerical coefficient evaluated for $p = 2.5$. These fiducial values correspond to $\nu F_\nu \approx 1.6 \times 10^{-15}$ erg cm$^{-2}$ s$^{-1}$ at $h\nu = 1$ keV for $\nu > \nu_c$, $\nu_m$ after one day, which is consistent with the *Chandra* upper limit (Margutti et al. 2017) of $F_X < 1.4 \times 10^{-15}$ erg cm$^{-2}$ s$^{-1}$ (0.3–10 keV) at 2.3 days. The corresponding optical magnitude for $\nu_m < \nu < \nu_c$ after one day is $R \sim 29$, which would be extremely hard to detect. The radio upper limit of $F_{10\,\rm GHz} < 15.4\,\mu$Jy at 1.39 days (Hallinan et al. 2017) is quite constraining here (a factor of ≈13 below the flux from Equation (7) for our fiducial values) and favors lower values of $n_0$ and/or $\epsilon_B$. Therefore, even if such material along the line of sight produces the observed GRB prompt emission, its afterglow emission would be very challenging to detect.

## 4. The Remnant of the NS–NS Merger

The type of remnant that was produced during this NS–NS merger is rather uncertain. The chirp mass was determined from the GW signal to be $\mathcal{M} \equiv (M_1M_2)^{3/5}(M_1+M_2)^{-1/5} = 1.188^{+0.004}_{-0.002}\,M_\odot$ (Abbott et al. 2017b), where $M_1$ and $M_2$ are the pre-merger (gravitational) masses of the two NSs. Figure 3 shows $M_1$ and $M_2$ as a function of their mass ratio, $q \equiv M_1/M_2 \leqslant 1$, along with the initial, pre-merger total mass of the system, $M_i = M_1 + M_2$. This measured chirp mass $\mathcal{M}$ implies $M_i \geqslant 2.73\,M_\odot$. The final mass, $M_f$, of the remnant that was left after the merger can, however, be smaller (by about ≈7%; Timmes et al. 1996) due to mass ejection and energy losses to gravitational waves and neutrinos during or shortly after the merger. Therefore, Figure 3 also shows an estimate of the resulting final mass $M_f$ after such a reduction (dashed magenta lines) by assuming that 0.01 $M_\odot$ (thick line) or 0.1$M_\odot$

(thin line) of baryonic mass was ejected during the merger, and using the relation between the baryonic ($M_b$) and gravitational ($M_g$) masses from Timmes et al. (1996), $M_b = M_g + 0.075M_g^2$ in solar masses.

The merger outcomes can be one of the following, in order of increasing remnant mass: a stable NS, a supra-massive NS (SMNS; e.g., Piro et al. 2017), an HMNS, or a BH. An SMNS is supported against collapse to a BH by uniform rigid-body rotation, and therefore typically collapses to a BH only on the order of its spindown time $\tau_{\rm sd}$ due to magnetic dipole braking. An HMNS is supported against collapse to a BH instead by differential rotation, and has an expected lifetime of $t_{\rm HMNS} \lesssim 1$ s before collapsing to a BH due to the relatively fast damping of differential rotation.

The exact range of final masses that corresponds to each of these outcomes is uncertain and depends on the equation of state (EOS). Nonetheless, it is evident that a stable NS remnant in GRB 170817A would require both approximately equal masses of the merging NSs, as well as a very stiff EOS. The GW signal does not strictly rule out the formation of an HMNS (Abbott et al. 2017d), which is the most likely outcome if indeed the collapse to a BH was delayed.

A massive NS formed in a binary NS merger would have a near break-up initial spin period of $\lesssim$1 ms, which corresponds to a very large initial rotational energy, $E_{\rm rot} \sim 10^{52.5}$–$10^{53}$ erg. This energy is channeled primarily into a pulsar-type ultra-relativistic MHD wind through magnetic dipole braking, and most of it is lost over $\tau_{\rm sd}$. For a long-lived (>2 s) massive NS remnant, namely, a stable NS or an SMNS (and possibly a particularly long-lived HMNS), it is not clear what powers the GRB 170817A since $\tau_{\rm sd} \gtrsim 10^2$ s even for a magnetar-strength magnetic field ($\sim 10^{15}$ G). An even stronger dipole field ($\gtrsim 10^{16}$ G) is needed to give $\tau_{\rm sd} < 2$ s, and then most of $E_{\rm rot}$ would be promptly channeled into the relativistic wind. Moreover, $\tau_{\rm sd}$ does not exceed several years even for a typical pulsar-like surface magnetic dipole field strength ($\sim 10^{12}$ G), and therefore by the time of the radio to X-ray observations within the first month after the event, at least a few percent of $E_{\rm rot}$, i.e., $\gtrsim 10^{51}$ erg (and possibly most of $E_{\rm rot}$) is extracted. Such an energy in a roughly isotropic relativistic wind is expected to produce a very bright afterglow emission as it interacts with the external medium, especially at a nearby distance of ≈40 Mpc, which is inconsistent with the multi-wavelength follow-up observations of GRB 170817A (Abbott et al. 2017c). Therefore, a stable NS or an SMNS remnant are highly unlikely.

This leaves either an HMNS or a direct formation of a BH. An HMNS could naturally account for the observed delay $\Delta t$ through $t_{\rm HMNS}$ as well as $t_{\rm bo}$ as the jet would need to bore its way through ∼1 s worth of neutrino-driven wind and dynamical ejecta propagation, whereas for a direct BH formation $t_{\rm HMNS} = 0$ and $t_{\rm bo}$ would likely be much shorter as the jet starts very shortly after the disk wind and dynamical ejecta. A BH would also require a relatively soft EOS. Hence, arguably, the most likely option appears to be the formation of an HMNS with a lifetime $t_{\rm HMNS} < \Delta t \approx 1.74$ s so that its collapse to a BH and subsequent accretion onto this BH could launch the jet that powered GRB 170817A, and still be consistent with the GRB's delayed onset with respect to the GW chirp signal (also see Margalit & Metzger 2017 for additional arguments favoring the formation of an HMNS).

## 5. Discussion

We have addressed some implications of GRB 170817A observations, combining its EM emission and the associated GW signal of the binary NS merger that triggered it—the first of its kind. In Section 2, we have used the observed time delay of $\Delta t = 1.74 \pm 0.05$ s between the GW chirp signal and the GRB onset in order to set an upper limit on the prompt GRB emission radius $R_\gamma \leqslant R_{\gamma,\rm max} \approx 2c\Delta t/\Delta\theta^2$ for a uniform jet with sharp edges viewed from outside of its aperture (see Equation (2) and Figures 1 and 2).

Next, in Section 3, we interpreted the relatively low measured values of $E_{\gamma,\rm iso}$ and $E_{\rm p}$ for GRB 170817A in the context of a narrow GRB jet viewed off-axis, from outside of its initial aperture. For a uniform sharp-edged jet this suggests that our line of sight is only slightly outside of the jet $\Delta\theta \sim (0.05 - 0.1)(\Gamma/100)^{-1}$, which would in turn imply an unusually high on-axis $E_{\rm p}(0) \sim$ 3–8 MeV (or ∼5–20 MeV for the main spike) and a relatively high $R_{\gamma,\rm max}$. The implied high $E_{\rm p}(0)$ and the expected afterglow lightcurves both favor an alternative picture (case (iii)), in which our viewing angle is larger ($\theta_{\rm obs} \gtrsim 2\theta_0$) and the prompt emission arises from material along our line of sight that is less energetic than the jet's core. This picture implies a higher afterglow flux at very early times, keeps GRB 170817A well above the Amati relation ($E_{\rm p} - E_{\gamma,\rm iso}$ correlation), like most SGRBs, and induces no angular time delay $t_\theta$. Since the radial time delay $t_r$ is typically negligible for a highly relativistic outflow, the observed delay $\Delta t \approx 1.74$ s would then likely be dominated by $t_{\rm HMNS} \gtrsim 1$ s and $t_{\rm bo} \sim 0.5$ s. A possible alternative is a mildly relativistic outflow along our line of sight (e.g., from a cocoon that breaks out) for which $\Delta t$ may be dominated by $t_r$.

The latter conclusion is consistent with the arguments raised in Section 4 against a long-lived massive NS remnant (stable NS or SMNS). While a direct formation of a black hole might still be possible, given the system's expected final mass this would not be the case for many of the leading models for the NS equation of state (e.g., Abbott et al. 2017a). Moreover, it would require another origin for the delay time $\Delta t$, such as the radial time delay $t_r$ for a mildly relativistic outflow. Nonetheless, the relatively large ejected mass ($\sim 0.05\,M_\odot$) that was inferred from detailed modeling of the kilonova emission (e.g., Drout et al. 2017; Evans et al. 2017; Kasen et al. 2017; Kasliwal et al. 2017; Kilpatrick et al. 2017; Pian et al. 2017; Smartt et al. 2017) favors relatively small values for the mass ratio, $q \lesssim 0.5$–$0.6$ for stiff EOSs (e.g., Rosswog et al. 2014; Sekiguchi et al. 2016; Ciolfi et al. 2017; Dietrich et al. 2017), which in turn would imply a larger total mass (see Figure 3) that would generally more easily lead to a direct BH formation. However, the required stiff EOSs for this effect to be important also imply a higher mass threshold for direct BH formation. Finally, if the BH and GRB jet form immediately following the NS–NS merger, then there would be very little neutrino-driven wind in front of the jet's head that would cause a significant fraction of its energy to be channeled into a cocoon, whose breakout might account for such a mildly relativistic outflow along our line of sight. These arguments appear to favor the formation of a short-lived HMNS, with a lifetime of $t_{\rm HMNS} \sim 1$ s or so.

The first detection of a GW signal from the merger of an NS–NS system was observed in coincidence with GRB 170817A. We were apparently lucky in the sense that most NS–NS merger GW signals are expected without an

associated GRB, since GRB jets are thought to be narrowly collimated, covering only a small fraction, $f_b \sim 10^{-2}$–$10^{-1}$, of the total solid angle. On the other hand, the evidence for narrow jets in short-hard GRBs is much weaker than in long-soft GRBs, so it might be that the beaming factor $f_b$ is larger than expected, which would require us to be somewhat less lucky to have observed the association with GRB 170817A. Moreover, it appears that our viewing angle $\theta_{\rm obs}$ is not particularly small (since most of the solid angle is at large angles), but the jet does not have sharp edges as is often assumed mainly out of convenience, but instead has wide wings that extend out to large angles from its symmetry axis. In this case, the prompt GRB emission in GRB 170817A was from such material with a low $E_{\rm k,iso} \sim E_{\gamma,\rm iso}$. A determination of $\theta_{\rm obs}$ from the GW signal together with elaborate multi-wavelength afterglow observations could help determine the GRB jet's angular structure, as well as constrain the prompt GRB emission radius $R_\gamma$.

J.G. and R.G. are supported by the Israeli Science Foundation under grant No. 719/14. R.G. is supported by an Open University of Israel Research Fellowship.

## ORCID iDs

Jonathan Granot https://orcid.org/0000-0001-8530-8941
Ramandeep Gill https://orcid.org/0000-0003-0516-2968

## References

Abbott, B. P., Abbott, R., Abbott, T. D., et al. 2016a, PhRvL, 116, 061102
Abbott, B. P., Abbott, R., Abbott, T. D., et al. 2016b, ApJ, 832, 21
Abbott, B. P., Abbott, R., Abbott, T. D., et al. 2017a, ApJL, 848, L13
Abbott, B. P., Abbott, R., Abbott, T. D., et al. 2017b, PhRvL, 119, 161101
Abbott, B. P., Abbott, R., Abbott, T. D., et al. 2017c, ApJL, 848, L12
Abbott, B. P., Abbott, R., Abbott, T. D., et al. 2017d, arXiv:1710.09320
Alexander, K. D., Berger, E., Fong, W., et al. 2017, ApJL, 848, L21
Baumgarte, T. W., Shapiro, S. L., & Shibata, M. 2000, ApJL, 528, 29
Berger, E. 2014, ARA&A, 52, 43
Bromberg, O., Tchekhovskoy, A., Gottlieb, O., Nakar, E., & Piran, T. 2017, arXiv:1710.05897
Ciolfi, R., Kastaun, W., Giacomazzo, B., et al. 2017, PRD, 95, 063016
Dietrich, T., Ujevic, M., Tichy, W., Bernuzzi, S., & Brugmann, B. 2017, PRD, 95, 024029
Drout, M. R., Piro, A. L., Shappee, B. J., et al. 2017, Sci, doi:10.1126/science.aaq0049
Eichler, D., & Granot, J. 2006, ApJL, 641, L5
Eichler, D., Livio, M., Piran, T., & Schramm, D. N. 1989, Natur, 340, 126
Evans, P. A., Cenko, S. B., Kennea, J. A., et al. 2017, Sci, doi:10.1126/science.aap9580
Gottlieb, O., Nakar, E., Piran, T., & Hotokezaka, K. 2017, arXiv:1710.05896
Granot, J., & Kumar, P. 2003, ApJ, 591, 108
Granot, J., & Ramirez-Ruiz, E. 2012, in Gamma-Ray Bursts, ed. C. Kouveliotou, S. E. Woosley, & R. A. M. J. Wijers (Cambridge: Cambridge Univ. Press), chap. 11 (arXiv:1012.5101)
Granot, J., & Sari, R. 2002, ApJ, 568, 820
Granot, J., Gill, R., Guetta, D., & De Colle, F. 2017, MNRAS, submitted (arXiv:1710.06421)
Granot, J., Panaitescu, A., Kumar, P., & Woosley, S. E. 2002, ApJL, 570, L61
Granot, J., Ramirez-Ruiz, E., & Perna, R. 2005, ApJ, 630, 1003
Haggard, D., Nyak, M., Ruan, J. J., et al. 2017, ApJL, 848, L25
Hallinan, G., Corsi, A., Mooley, K. P., et al. 2017, Sci, doi:10.1126/science.aap9855
Ioka, K., & Nakamura, T. 2017, arXiv:1710.05905
Jin, Z-P., Li, X., Wang, H., et al. 2017, arXiv:1708.07008
Kasen, D., Metzger, B., Barnes, J., Quataert, E., & Ramirez-Ruiz, E. 2017, Natur, 551, 80
Kasliwal, M. M., Nakar, E., Singer, L. P., et al. 2017, Sci, doi:10.1126/science.aap9455
Kathirgamaraju, A., Barniol Duran, R., & Giannios, D. 2017, arXiv:1708.0748
Kilpatrick, C. D., Foley, R. J., Kasen, D., et al. 2017, Sci, doi:10.1126/science.aaq0073
Lazzati, D., Deich, A., Morsony, B. J., & Workman, J. C. 2017a, MNRAS, 471, 1652
Lazzati, D., Lopez-Camara, D., Cantiello, M., et al. 2017b, ApJL, 848, L6
Margalit, B., & Metzger, B. D. 2017, ApJL, 850, L19
Margutti, R., Berger, E., Fong, W., et al. 2017, ApJL, 848, L20
Moharana, R., & Piran, T. 2017, MNRAS, 472, L55
Murguia-Berthier, A., Ramirez-Ruiz, E., Kilpatrick, C. D., et al. 2017, ApJL, 848, L34
Nakar, E. 2007, PhR, 442, 166
Nakar, E., & Piran, T. 2017, ApJ, 834, 28
Nakar, E., Piran, T., & Granot, J. 2002, ApJ, 579, 699
Narayan, R., Paczynski, B., & Piran, T. 1992, ApJL, 395, L83
Pian, E., D'Avanzo, P., Benetti, S., et al. 2017, Natur, 551, 67
Piro, A. L., Bruno, G., & Perna, R. 2017, ApJ, 844L, 19
Rosswog, S., Korobkin, O., Arcones, A., Thielemann, F.-K., & Piran, T. 2014, MNRAS, 439, 744
Rosswog, S., Piran, T., & Nakar, E. 2013, MNRAS, 430, 2585
Salafia, O. S., Ghisellini, G., Pescalli, A., et al. 2015, MNRAS, 450, 3549
Sekiguchi, Y., Kiuchi, K., Kyutoku, K., Shibata, M., & Taniguchi, K. 2016, PRD, 93, 124046
Smartt, S. J., Chen, T.-W., Jerkstrand, A., et al. 2017, Natur, 551, 75
Timmes, F. X., Woosley, S. E., & Weaver, T. A. 1996, ApJ, 457, 834
Troja, E., Piro, L., van Eerten, H., et al. 2017, Natur, 551, 71
von Kienlin, A., Meegan, C., & Goldstein, A. 2017, GCN, 21520
Woosley, S. E., & Bloom, J. S. 2006, ARA&A, 44, 507